Electronic Supplementary Information

Recyclable ferroferric oxide@titanium dioxide@molybdenum disulfide with enhanced enzyme-like activity under visible light for effectively inhibiting drug-resistant bacteria in sewage

Yiping Sun, [#,a] Wenhui Yue, [#,a] Bin Niu, [b] Yu Lin, [c] Xiangyong Liu, [c] Tianming Wu, [a] Gong Zhang, [d] Ke Qu, [*,e] Lu Wang, [*,a] and Yusheng Niu [*,a,e]

[a] Institute of Biomedical Engineering, College of Life Sciences, Qingdao University, Qingdao 266071, China

[b] Jinan Art School, Jinan 250002,China

[c] Yantai Center for Disease Control and Prevention, Yantai 264003, China

[d] Center for Water and Ecology, State Key Joint Laboratory of Environment Simulation and Pollution Control, School of Environment, Tsinghua University, Beijing 100084, China

[e] College of Materials and Chemistry & Chemical Engineering, Chengdu University of Technology, Chengdu 610059, China

[f] School of Tourism and Geography Science, Qingdao University, Qingdao 266071, China

[#] Yiping Sun and Wenhui Yue contributed equally to this work.

*Correspondence: quke18@cdut.edu.cn (K. Qu); LWang@qdu.edu.cn (L. Wang); nys@qdu.edu.cn (Y. Niu)

S1. Kinetic and reaction mechanism of the peroxidase-like activity of Fe_3O_4@TiO_2@MoS_2

The kinetic parameters and reaction mechanism of the POD-like behavior of Fe_3O_4@TiO_2@MoS_2 were studied using the Michaelis equation. Kinetics study were performed in the acetate buffer (100 mM, pH 4.0) with the final concentration of H_2O_2 (5 mM) and various concentrations of TMB (0.1–1.8 mM) or with the final concentration of TMB (1 mM) and diverse concentrations of H_2O_2 (0.06–0.5 mM). The values of Vmax and Km were evaluated by the Equation (1), where [S], Km, V, and Vmax are the substrate's concentration, Michaelis constant, initial velocity, and the maximal reaction velocity, respectively.

$$V = \frac{V_{max} \times [S]}{V_m + [S]} \quad (1)$$

Statistical analysis: All data are shown as mean ± s.d.

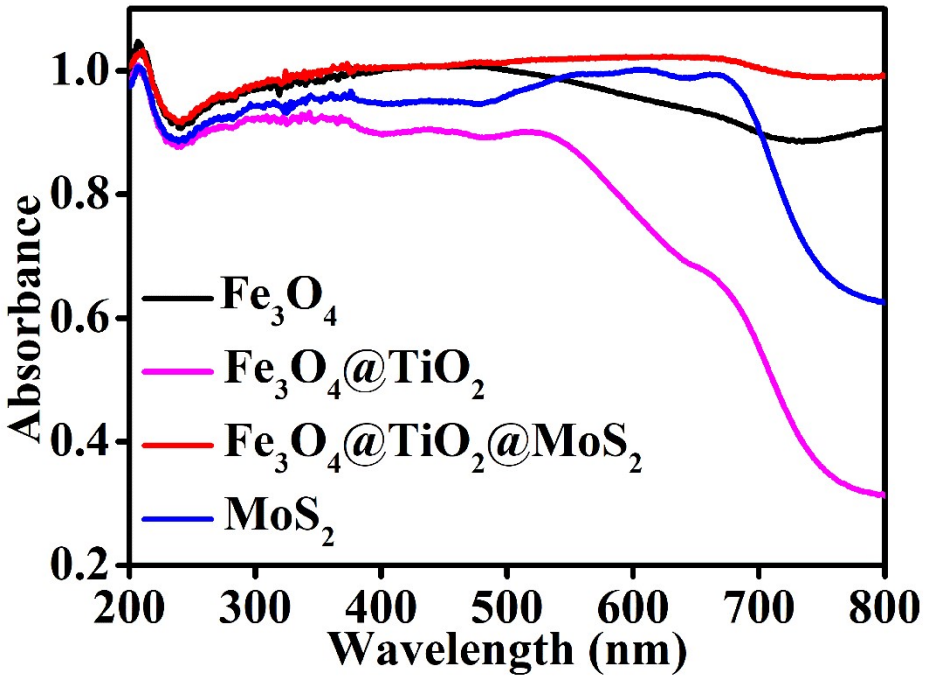

Fig. S1. UV–vis diffuse reflectance spectra of Fe_3O_4, Fe_3O_4@TiO_2, Fe_3O_4@TiO_2@MoS_2, and MoS_2.

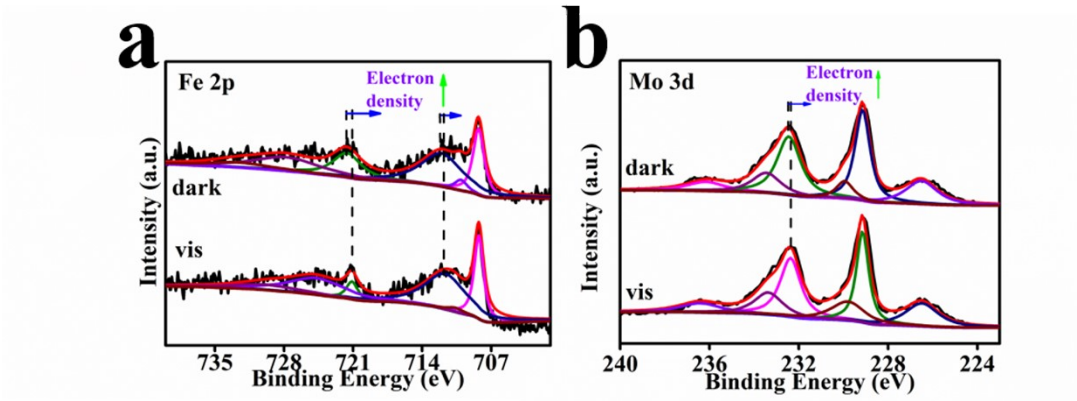

Fig. S2. High-resolution XPS for Fe 2p (a) and Mo 3d (b) of Fe_3O_4@TiO_2@MoS_2 in the dark (Fe_3O_4@TiO_2@MoS_2 (Dark)) or under the visible light irradiation from the Xe lamp with a 430 nm cutoff filter (Fe_3O_4@TiO_2@MoS_2 (Vis)).

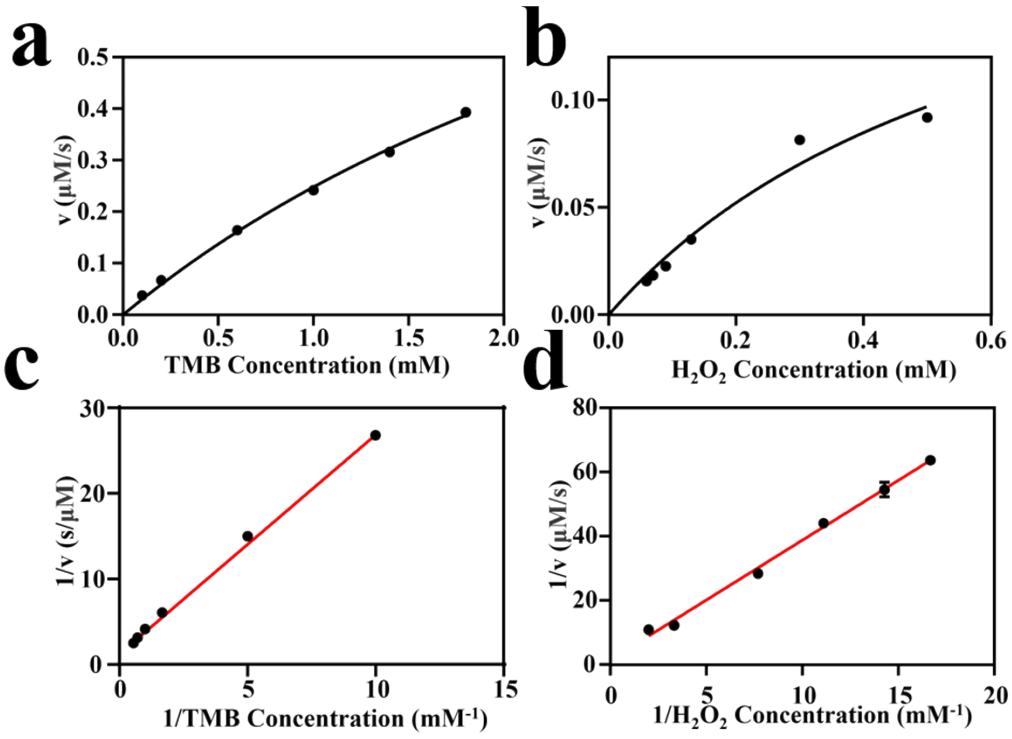

Fig. S3. Steady-state kinetics of the peroxidase-like activity of the Fe_3O_4@TiO_2@MoS_2.

a, c) The concentration of H_2O_2 was fixed, and the concentration of TMB changed; b, d) The concentration of TMB was fixed and the concentration of H_2O_2 changed; The error bars represent the standard deviation for three measurements (n = 3).

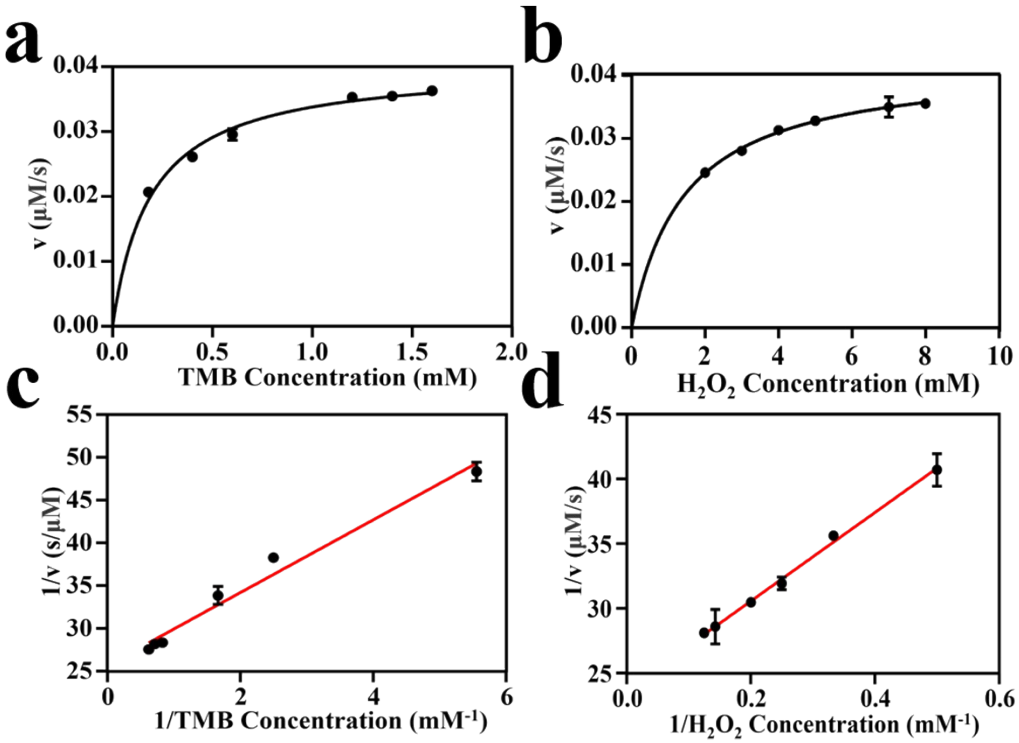

Fig. S4. Steady-state kinetics of the peroxidase-like activity of the MoS_2. a, c) The concentration of H_2O_2 was fixed, and the concentration of TMB changed; b, d) The concentration of TMB was fixed and the concentration of H_2O_2 changed; The error bars represent the standard deviation for three measurements (n = 3).

Fig. S5. (a) The magnetic hysteresis loops of Fe_3O_4(I), Fe_3O_4@TiO_2(II), and Fe_3O_4@TiO_2@MoS_2(III) and (b) physical drawing of magnetic separation of Fe_3O_4@TiO_2@MoS_2.

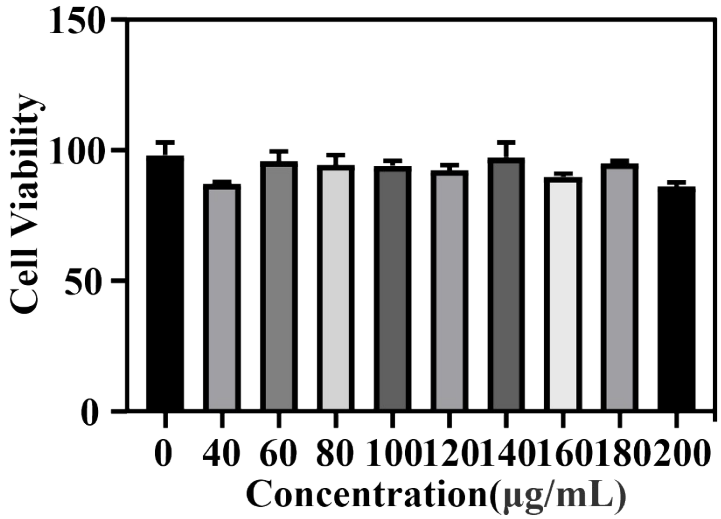

Fig. S6. MTT cytotoxicity assay: The viability of L929 cells treated with different sizes of Fe_3O_4@TiO_2@MoS_2 was used as an example. Error bars indicate the standard deviation of the three measured values (n = 3).

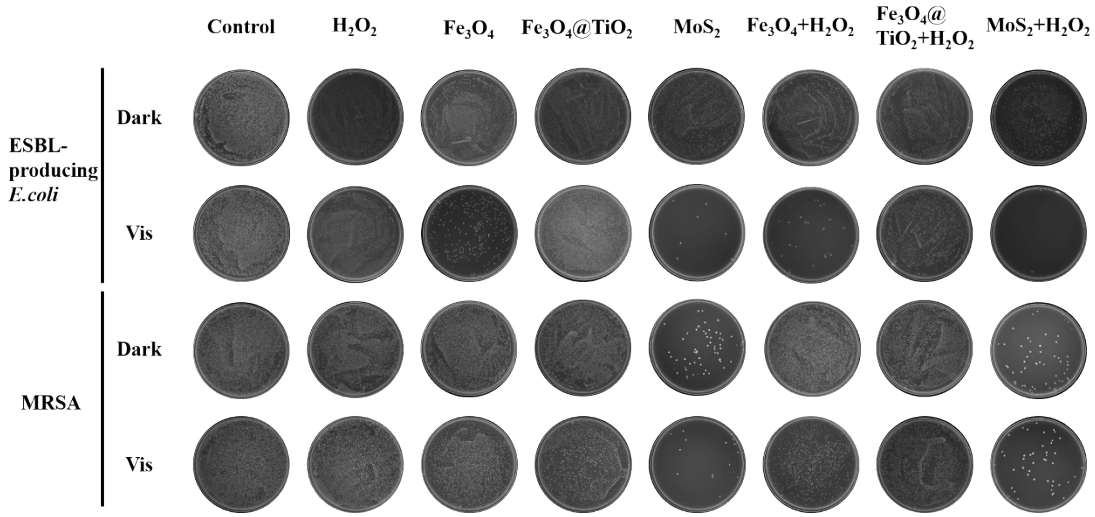

Fig. S7. Colony plots of the inhibition effect of different treatments on ESBL-producing *E. coli* and MRSA.

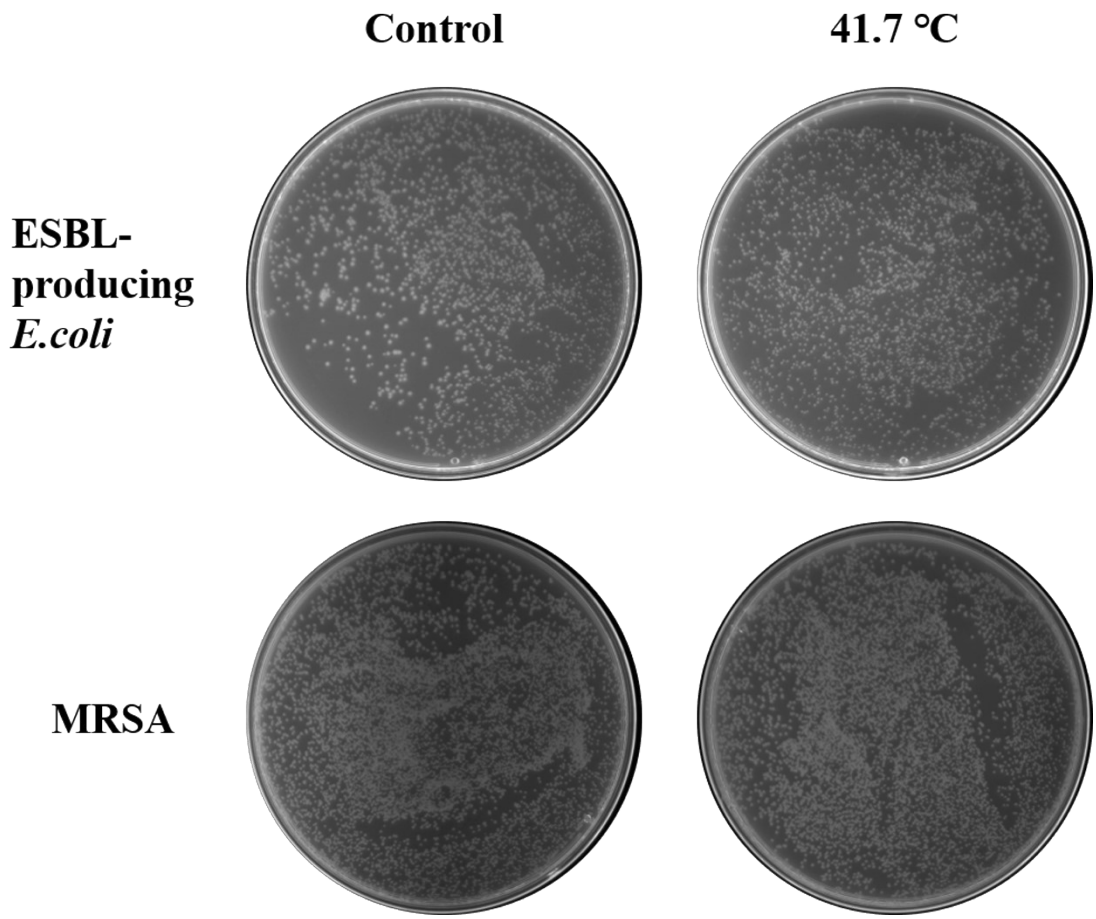

Fig. S8. Colony diagram of the inhibition effect of low-temperature treatment on ESBL-producing *E. coli* and MRSA.

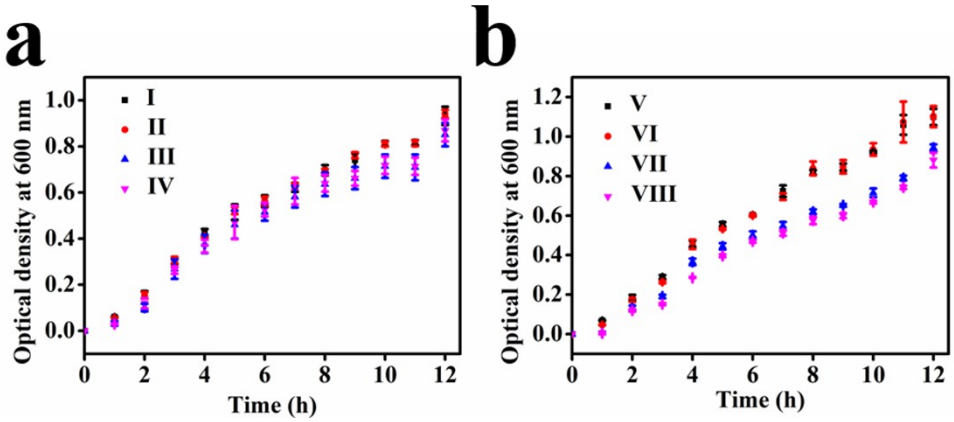

Fig. S9. The growth curves of MRSA under (a) dark conditions and (b) visible light irradiation. Cultured bacterial cells were treated with (I/V) Sterile water as control,

(II/VI) H_2O_2, (III/VII) Fe_3O_4@TiO_2@MoS_2, and (IV/VIII) Fe_3O_4@TiO_2@MoS_2+H_2O_2.

Table S1. Comparison of Michaelis-Menten constants (K_m) and maximum initial reaction rates (V_{max}) of the oxidation reaction catalyzed by Fe_3O_4@TiO_2@MoS_2, MoS_2, HRP, TiO_2@CeOx, Fe_3S_4, and GO-COOH.

Catalyst	K_m (mM)		V_{max} (10^{-7} M/s)		References
	H_2O_2	TMB	H_2O_2	TMB	
Fe_3O_4@TiO_2@MoS_2	**0.6678**	**4.184**	**2.264**	**12.86**	**This work**
MoS_2	**1.442**	**0.1923**	**0.4216**	**0.4027**	**This work**
HRP	**3.7**	**0.434**	**0.871**	**1**	[1]
TiO_2@CeO_x	**1.39**	**0.3**	**0.55**	**0.12**	[2]
Fe_3S_4	**1.158**	**0.160**	**21.68**	**11.46**	[3]
GO-COOH	**3.99**	**0.0237**	**38.5**	**34.5**	[4]
MoO_{3-X} DNs	**0.26**	**2.65**	**1.52**	**0.0152**	[5]

References

1. L. Gao, J. Zhuang, L. Nie, J. Zhang, Y. Zhang, N. Gu, T. Wang, J. Feng, D. Yang, S. Perrett and X. Yan, *Nat Nanotechnol*, 2007, **2**, 577-583.
2. L. Artiglia, S. Agnoli, M. C. Paganini, M. Cattelan and G. Granozzi, *ACS Appl Mater Interfaces*, 2014, **6**, 20130-20136.
3. C. Ding, Y. Yan, D. Xiang, C. Zhang and Y. Xian, *Microchimica Acta*, 2015, **183**, 625-631.
4. Y. Song, K. Qu, C. Zhao, J. Ren and X. Qu, *Adv Mater*, 2010, **22**, 2206-2210.
5. Y. Zhang, D. Li, J. Tan, Z. Chang, X. Liu, W. Ma and Y. Xu, *Small*, 2021, **17**, e2005739.